NASA

Technical Memorandum 80247

Observations of the Transient X-Ray Source 4U0115 + 63

(NASA-TM-80247) OBSERVATIONS OF THE TRANSIENT X-RAY SOURCE 4U0115+63 (NASA) 25 p HC A02/MF A01 CSCL 03A N79-20947

Unclas
G3/89 19652

L. A. Rose, S. H. Pravdo, L. J. Kaluzienski, F. E. Marshall, S. S. Holt, E. A. Boldt, R. E. Rothschild and P. J. Serlemitsos

MARCH 1979

National Aeronautics and Space Administration

Goddard Space Flight Center
Greenbelt, Maryland 20771

OBSERVATIONS OF THE TRANSIENT X-RAY SOURCE 4U0115+63

L.A. Rose*, S.H. Pravdo**, L.J. Kaluzienski***, F.E. Marshall*,
S.S. Holt, E.A. Boldt, R.E. Rothschild****, and P.J. Serlemitsos

Laboratory for High Energy Astrophysics
NASA/Goddard Space Flight Center
Greenbelt, Maryland 20771

ABSTRACT

We present results of HEAO-A2 pointed observations and Ariel V All Sky Monitor observations of the X-ray transient 4U0115+63. The transient source pulses with a period of 3.6136 s ± .0004 s, has a hard spectrum typical of an X-ray binary pulsar, and has a broad iron line emission feature. A discussion of the transient behavior is given and inferences are made concerning the nature of the X-ray source based on the pointed data.

* NAS/NRC Research Associate

** Also Department of Physics and Astronomy, Univ. of Maryland

*** Now at NASA Headquarters, Washington, D.C.

**** Now with UCSD

I. INTRODUCTION

The transient X-ray source 4U0115+63 displayed a rapid increase in brightness in late December 1977 and January 1978 as reported by SAS-3 and Ariel V observers (Cominsky _et al_. 1978a; Holt and Kaluzienski 1978). Clark and Cominsky (1978) discovered that it pulsates with a 3.6 second period. This is the third transient to exhibit pulsations, the other two being A1118-61 (Ives _et al_. 1975) and A0535+26 (Rosenberg _et al_. 1975). Based on Doppler variations of the pulse period, Rappaport _et al_. (1978a) found that 4U0115+63 is in a binary system with a period of 24 days. On 16 January 1978 the HEAO-1 observatory pointed at this source for 3 hours (2 orbits of the satellite). This paper presents results of pulse-phase spectral analysis from the HEAO-A2 experiment and observations of the transient behavior by the Ariel 5 All Sky Monitor (ASM).

II. EXPERIMENT AND ANALYSIS

The All-Sky Monitor aboard Ariel V is a pinhole camera sensitive to X-rays in the 3-6 keV energy range. It has an effective area of 0.6 cm^2 with a duty cycle of $\sim$ 1% for a given source and monitors more than 3π of the celestial sphere each orbit. A complete description of the Ariel V All Sky Monitor is given by Holt (1976).

Six gas-filled proportional counters comprise the HEAO-A2 experiment[+]. Two low energy detectors cover the energy range 0.15 - 3 keV; one medium energy detector (MED) filled with argon gas is sensitive in the 1.5 - 15 keV energy range; and three xenon gas-filled high energy detectors (HED)

[+]The HEAO A2 experiment is a collaborative effort led by E. Boldt of GSFC and G. Garmire of CIT, with collaborators at GSFC, CIT, JPL and UCB.

operate in the 2 - 60 keV energy range. A detailed description of the A2 experiment aboard HEAO-1 is given by Rothschild et al. (1978). During the point HED II observed the source intensity with 80 msec resolution while the MED and HED III operated in a real time mode, recording the arrival time and measuring the energy of individual events. The X-ray background was determined from scans of source-free regions of the sky during the days immediately before the point. A pulse period of 3.6136 s ± .0004 s, consistent with the period given by Cominsky et al. (1978b), was determined from the HEAO-A2 pointed data; the MED and HED III data were folded modulo this period and accumulated in bins one-tenth pulse period wide, using January 16.0 as the reference time (see Figure 2). The number of events in each bin was approximately 8500. The spectral analysis utilizes a technique in which model spectra are multiplied by the detector response matrix and compared to the net PHA data using a χ^2 test. Inferred incident spectra are then obtained by dividing the PHA data by spectrum-dependent channel-by-channel efficiencies (see Figure 3). Additional information about the method of spectral analysis has been given by Serlemitsos et al. (1975) and by Pravdo et al. (1978).

For pulse-phase analysis two analytic forms were used to fit the data. They were a) a power law model of the form

$$\frac{dN}{dE} \text{ (photons cm}^{-2}\text{ sec}^{-1}\text{ keV}^{-1}) = P_1 E^{-P_2} \text{ for } E \leq P_3$$

and

$$\frac{dN}{dE} = P_1 E^{-P_2} \text{ EXP } \left(-\frac{(E-P_3)}{P_4}\right) \text{ for } E > P_3,$$

and b) a blackbody model for which

$$\frac{dN}{dE} = C \cdot E^2/(\text{EXP}(E/KT)-1).$$

In the power law model a high energy cutoff factor was used beginning at $E = P_3$ with an e-folding energy P_4. The power law model and the parameter notation used here were also employed by Pravdo et al. (1978) in analyzing Hercules X-1 spectra. A similar power law model was used by Becker et al. (1978) to describe the continuum of Vela X-1. In general thermal bremsstrahlung fits were less good than were power law or black-body hypotheses in fitting the data.

III. RESULTS

The ASM light curve for the 1978 outburst of 4U0115+63 is shown in Figure 1. The data represent $\sim 1/2^d$ averages of the incident 3-6 keV photon flux with corresponding 1σ statistical errors. As seen from this figure, the present episode is characterized by a rise phase lasting $\sim 10^d$ to a level of $\sim 1/2$ that of the Crab nebula and subsequent slower decline (e-folding time $\sim 20^d$) back to the pre-flare intensity ($S \lesssim 0.08\ S_{Crab}$). While variations on shorter time scales are evident (cf. days 11-15), no significant decreases in the X-ray flux are observed near the predicted times of superior conjunction on 9 January and 1 February (Rappaport et al. 1978b), consistent with SAS-3 observations covering the latter interval (Rappaport et al. 1978b). Also indicated in Figure 1 are the times of A2 pointed and scanning mode observations of 4U0115+63 during the outburst.

Figures 2a and 2d show the 2 - 60 keV integrated energy curves (from the HEAO-A2 pointed data) as a function of pulse phase for HED III and MED. The pulse has a main intensity peak in bin 8 and a secondary peak in bin 1. This pulse profile including the weak secondary peak is similar to that reported by Johnston et al. (1978). For the HED III data the power law model gave a better χ^2 fit than did the blackbody model for all parts of the pulse; however, in bins 3, 4, and 5 the power law fit was only slightly better than the blackbody fit. Figure 2b shows that the power law index changes across the pulse, the change between bins 2 and 3 being particularly great. The lack of fine temporal resolution (i.e., the pulse was divided into only 10 bins) prohibits seeing the evolution of the spectrum between these two bins. Throughout the pulse the spectra are very hard, the spectrum of bin 3 being the hardest with a power law number index, $\alpha \sim 0.1$. The cutoff and folding parameters are shown in Figure 2c. Figures 2e and 2f show how the model parameters change across the pulse for the MED spectra. While the values are not exactly the same as for the HED III spectra the same general trends are evident across the pulse. Bin 3 has the hardest spectrum and there is also some evidence for spectral hardening in bin 8 of the MED data and in bin 9 of the HED data. This is not as statistically significant as the hardening in bin 3 which is clearly present in spectra from both detectors.

Figure 3 shows HED III spectra for bins 2 and 3. These spectra exhibit the extreme value of power law indices found across the pulse. In the energy range above 30 keV there is a tendency for the data points to lie above the continuum. However, the large statistical uncertainties associated with the data points and the uncertainty in the true position of the continuum for this portion of the curve make the identification of features difficult. The shoulder or line seen in bin 2 of Fig. 3 is present (to a lesser extent) in bins 1, 3, 4 and 6 but this excess is not found in bins 7, 8, 9, and 10, the portion of the pulse that includes the main peak of the pulse intensity profile. Subtraction of OFF-pulse data (bins 1+2+3+4+5+6) from ON-pulse data (bins 7+8+9+10) would yield a curve with a feature near 11.5 keV (Rose et al. 1978) having the appearance of an absorption dip. It is thought that this is an artifact of the process of subtracting two inferred spectra (Pravdo et al. 1979); although similar features have been interpreted by other authors as indicating the presence of either cyclotron emission or absorption (Trumper et al. 1977; Wheaton et al. 1978).

A blackbody (with no absorption) yielded acceptable fits to bins 3, 4, and 5 of the HED data with values of KT in the range from 2.7 to 2.81 keV (see Figure 4). Davidson and Ostriker (1973) have described cylindrical volumes (or hot spots) with height $\simeq$ radius, located at the magnetic poles near the surface of a neutron star, which are the source of X-ray emission. Using the observed intensity, the temperature from the blackbody model and a distance of 5 Kpc to the object, a value of 2 km for the radius of a hot spot and an X-ray luminosity of 2.6×10^{37} ergs/sec (2 - 60 keV) were determined. The distance of 5 kpc was estimated by Johnston _et al._ (1978) to account for the observed extinction of the optical counterpart which is thought to be either a B-type main-sequence or giant star (Johns _et al._ 1978). Using a distance of 2.5 kpc to 4U0115+63 calculated by Rappaport _et al._ (1978b), the values for the hot spot radius and X-ray luminosity are 1 km and 7×10^{36} ergs/sec respectively. Therefore the observations imply that the size of the X-ray emitting region is smaller than the typical 1 M_0 neutron star radius of $\sim$ 10 km, and that only a part of the neutron star surface may be producing the observed emission.

Neither a simple power law plus high energy cutoff nor a blackbody gave an acceptable χ^2 fit to the combined HED spectrum. This is not surprising since the power law index and cutoff parameters vary so much across the pulse. However, the addition of a broad iron line at ~6.6 keV to the power law model reduced χ^2 from 400 to 250 for 36 degrees of freedom. Similarly the addition of a broad iron line at 6.8 keV to the power law model fit of the combined MED spectrum reduced χ^2 from 300 to 70 for 33 degrees of freedom. These reductions in χ^2 have large statistical significance and are taken as evidence of iron line emission from 4U0115+63. The analytic form of the power law model used to fit the combined spectrum was the same as given in Part II with the addition of a Gaussian line profile and a factor, exp $(-N_H\sigma)$, where σ is the energy dependent absorption cross-section of cold matter and N_H is the equivalent hydrogen column density (Brown and Gould 1970, Fireman 1974).

Since the MED had more channels in the energy range of the iron line than did HED III, the line characteristics as determined from the MED spectral fit are given (see Table 1). The errors represent 70% confidence limits.

IV. DISCUSSION

The observed and inferred characteristics of 4U0115+63 including the 3.6 second pulsed X-ray emission, the 24 day binary period and a luminosity of $\sim 10^{37}$ ergs/sec are consistent with the model of a rotating neutron star in a binary system with the X-ray luminosity being powered by mass accretion onto the compact object (Davison and Ostriker 1973; Lamb et al. 1973).

In attempting to explain the intensity profile and spectral changes that occur in the pulse of Hercules X-1, Pravdo et al. (1977b) have proposed that the intensity profile arises from energy-independent scattering processes in the stellar atmosphere while the pulse spectral changes are due to elementary processes at or near the neutron star surface. The large change in spectral index in bins 2 and 3 of the pulse which occurs during a small change in intensity in these bins tends to support this model.

The high energy cutoff could be produced by cyclotron resonance absorption of an underlying continuum (Pravdo et al. 1978). In this model high momentum infalling electrons resonantly absorb photons as cyclotron line photons. This model is useful to show how certain parameters (e.g. the angle between the magnetic field direction and the line of sight to an observer) vary as a function of pulse phase. In the case of 4U0115+63 electron energies had to be relativistic in order to produce a cutoff beginning in the relatively low energy range of 8-10 keV with an acceptable χ^2 fit. This may not be a viable model in this case since other effects (e.g. pair production) could become important in this regime. Ross et al. (1978) have shown that Compton scattering of radiation in a cool gas surrounding a compact X-ray source can also produce a high energy cutoff. However, the variation of spectral parameters with pulse phase in the case of 4U0115+63 suggests a dependence on the angle between the line of sight to an observer and the polar magnetic field, even though there is a problem with the simple cyclotron resonance absorption model used here. This tends to rule out the Compton scattering model of Ross et al. (1978) since such a dependence is not expected.

A gas shell partially surrounding a neutron star has been suggested to account for X-ray pulsations and in particular to account for the intensity profile of the Her X-1 pulse (Basko and Sunyaev 1976a; McCray and Lamb 1976;

Basko and Sunyaev 1976b). Such a configuration might be applicable to this system as well. In this model the intensity variation of the pulse is due to absorption and collimation by the shell rather than anisotropic emission at the neutron star surface. In the McCray-Lamb model gaseous material is concentrated mostly around the magnetic equator and the magnetic poles (the magnetic dipole axis and the rotational axis do not coincide). This shell of gas is located at or near the Alfven radius. Processes occurring here could be independent of those occurring near the surface of the star. The McCray-Lamb model gives an intensity peak when the line-of-sight is close to the magnetic pole and a weaker secondary intensity peak when the line-of-sight is closest to the opposite pole. The strength of these intensity peaks could vary if the amount of absorbing material changes. Basko and Sunyaev (1976a) and McCray and Lamb (1976) have predicted a soft X-ray luminosity in the .1 - 1 keV energy range (comparable to the hard X-ray luminosity) from the gas shell surrounding the neutron star. Based on the observed B-V color of the B type companion star, for the 4U0115+63 system, given by Johns et al. (1978) and a relationship between number of equivalent H atoms/cm^2 and the interstellar reddening E_{B-V} (Ryter et al. 1975), we estimate the optical depth to range from $\sim$ 2 at 1 keV to $\sim$ 80 at .2 keV. These calculations suggest the soft X-ray luminosity for 4U0115+63 cannot be determined because of high extinction.

The iron line FWHM width based on an analysis of MED data is unusually large. A Doppler broadened iron line could be produced from fluorescing material in a rotating shell at the Alfven surface (Boldt 1977, Pravdo et al. 1977a). However, in the case of 4U0115+63, the large FWHM width implies that corotating material would have to extend to distances much larger than the radius for which such corotating material would be in Keplerian orbit, suggesting that this is not the source of line broadening. Alternatively, Ross et al. (1977) have shown that iron line features can be broadened due to Comptonization in a gas surrounding the X-ray source which is optically thick to Thomson scattering.

The long time scale variability of 4U0115+63 also provides some important information regarding the nature of this system. As evident in Figure 1, the present outburst closely resembles the characteristic variation exhibited by the transient X-ray sources. In addition, strong evidence for recurrence of the flares from this source is present in the long-term data record. Forman, Jones, and Tananbaum (1976) have reported a potentially similar flare from 4U0115+63 observed with the UHURU satellite during the period 1970 December - 1971 March. While it is difficult to compare in detail the present light curve (Figure 1) with the UHURU data (the latter consist of measurements occurring at irregularly spaced intervals ranging from days to weeks), it is interesting, nonetheless, that the 1971 observations are roughly consistent with a flare-like episode similar to the 1978 outburst. If the actual peak flux of the earlier event is comparable to the maximum measured UHURU value of $S \sim 0.07\ S_{crab}$ (as suggested by three measurements at that level over a one-week period, see Forman et al. 1976), a variable flare amplitude is implied. The lack of any detections of 4U0115+63 above the ASM threshold of $S_0 \approx 0.1\ S_{crab}$ during 1974 October - 1978 January probably does not meaningfully constrain the minimum recurrence interval, therefore, and we can conclude only that this interval is $\lesssim 7^y$. It thus appears likely that a significant fraction of the source emission is confined to low duty-cycle, recurrent outbursts of varying amplitude and duration, similar to the behavior of the recurrent transients A0535+26, Agl X-1, 4U1608-52, and 4U1630-47.

4U0115+63 is reminiscent of the Taurus transient A0535+26 (Rosenberg et al. 1975; Kaluzienski et al. 1975) in a number of respects. These include the relatively low energy output (low peak flux and/or rapid decay) and recurrent nature of the flares, extended low-level inter-flare emission, hard X-ray spectrum, exhibition of X-ray pulsations, and identification with early-type optical companions. In addition, some evidence exists that A0535+26 is also a member of a long-period binary system (Rappaport et al. 1976). A0535+26 and the transient X-ray pulsar in Centaurus, A1118-61 (Eyles et al. 1975), have been classified by Kaluzienski et al. (1977) as "Type II" transients primarily on the basis of their hard spectra, brief flare duration, and identification with massive, early-type optical counterparts. In contrast, sources categorized as "Type I" are characterized by a higher mean intensity, slower decline, soft flare spectrum, and identification with a low-mass, late-type optical counterpart, (cf. Kaluzienski 1977). The present observations thus support the identification of 4U0115+63 with the Type II transient source subset, as suggested by the SAS-3 timing observations (Cominsky et al. 1978b; Rappaport et al. 1978b). The most widely accepted explanation for the Type II outburst invokes a sudden increase in the accretion rate onto a collapsed object resulting from a sharp enhancement in the stellar wind or episodic mass transfer from a B emission star companion. Although the present spectral measurements of 4U0115+63 do not preclude the trnasient existence of a dense, screening stellar wind, the absence of substantial low energy absorption (orbital phase relative to superior conjunction of HEAO-1 pointed observation $\Phi \simeq 0.28$) or accretion wake-associated dips (Pounds et al. 1975) in the X-ray light curve suggest that mass exchange in the present case occurs via episodic equatorial ejection as commonly observed in B emission stars (Huang 1973; Maraschi et al. 1976). A similar conclusion was reached by Rappaport et al. (1978b) on the basis of the determination of a wide orbital separation in this binary. We note, however, that the stellar wind may play a significant role in producing the low-level quiescent X-ray emission reported from UHURU (Forman, Jones, and Tananbaum 1976) and OSO-7 (Markert 1974).

We thank R.H. Becker for helpful discussions; we also thank an anonymous referee for helpful comments.

REFERENCES

Amnuel, P. R., and Guseinov, O. Kh. 1976, Sov. Astron. Lett. 2, No. 4, 152.

Avni, Y., Fabian, A. C., and Pringle, J. E. 1976, M.N.R.A.S. 175, 297.

Basko, M. M. and Sunyaev, R. A. 1976a, M.N.R.A.S. 175, 395.

Basko, M. M. and Sunyaev, R. A. 1976b, Sov. Astron. 20, No. 5, 537.

Becker, R. H., Rothschild, R. E., Boldt, E. A. Holt, S. S., Pravdo, S. H., Serlemitsos, P. J. and Swank, J. H. 1978, Ap. J. 221, 912.

Boldt, E. 1977, Annals of the New York Academy of Sciences 302, 329.

Brown, R. L. and Gould, R. J. 1970, Phys. Rev. D1, 2252.

Clark, G. W., and Cominsky, L. 1978, IAU Circ. No. 3161.

Cominsky, L., Clark, G. W., Li, F., Mayer, W., and Rappaport, S. 1978a, IAU Circ. Nos. 3161, 3163.

Cominsky, L., Clark, G. W., Li, F., Mayer, W., and Rappaport, S. 1978b, Nature 273, 367.

Davidson, K., and Ostriker, J. P. 1973, Ap. J. 179, 585.

Eyles, C. J., Skinner, G. K., Willmore, A. P., and Rosenberg, F. D. 1975, Nature 254, 577.

Fireman, E. L. 1974, Ap. J. 187, 57.

Forman, W., Jones, C., and Tananbaum, H. 1976, Ap. J. (Letters) 206, L29.

Holt, S., and Kaluzienski, L. 1978, IAU Circ. No. 3161.

Holt, S. S. 1976, Ap. Space Sci. 42, 123.

Huang, S. 1973, Ap. J. 183, 541.

Ives, J., Sanford, P., and Bell Burnell, S. 1975, Nature 254, 578.

Johns, M., Koski, A., Canizares, C. and McClintock, J. 1978, IAU Circ. No. 3171.

Johnston, M., Bradt, H., Doxsey, R., Gursky, H., Schwartz, D., and Schwartz, J. 1978, Ap. J. (Letters) 223, L71.

Kaluzienski, L. J., Holt, S.S., Boldt, E. A., and Serlemitsos, P. J. 1975, Nature 256, 633.

Kaluzienski, L. J., Holt, S. S., Boldt, E. A., and Serlemitsos, P. J. 1977, Ap. J. 212, 203.

Kaluzienski, L. J. 1977, Ph.D. Thesis, University of Maryland.

Lamb, F. K., Pethick, C. J., and Pines, D. 1973, Ap. J. 184, 271.

Maraschi, L., Treves, A. and Van der Heuvel, E.P.J. 1976, Nature 259, 292.

Markert, T. 1974, Ph.D. Thesis, MIT.

McCray, R. and Lamb, F. K 1976, Ap. J. (Letters) 204, L115.

Pounds, K. A., Cooke, B. A., Ricketts, M. J., Turner, M. J., and Elvis, M. 1975, M.N.R.A.S. 172, 473.

Pravdo, S. H., Becker, R. H., Boldt, E. A., Holt, S. S., Serlemitsos, P. J., and Swank, J. H. 1977a, Ap. J. (Letters) 215, L61.

Pravdo, S. H., Boldt, E. A., Holt, S. S., and Serlemitsos, P. J. 1977b, Ap. J. (Letters) 216, L23.

Pravdo, S.H., Bussard, R. W., Becker, R. H., Boldt, E.A., Holt, S.S., and Serlemitsos, P.J. 1978, Ap. J. 225, 988.

Pravdo, S.H., White, N.E., Boldt, E.A., Holt, S.S., Serlemitsos, P.J., Swank, J.H., Tuohy, I., and Garmire, G. 1979, submitted to Ap. J.

Rappaport, S., Clark, G., Cominsky, L., and Li, F. 1978a, IAU Circ. No. 3171.

Rappaport, S., Clark, G. W., Cominsky, L., Joss, P. C., and Li, F. 1978b, Ap. J. (Letters) 224, L1.

Rose, L.A., Pravdo, S.H., Kaluzienski, L. J., Marshall, F. E., Holt, S. S., Boldt, E. A., Rothschild, R. E., and Serlemitsos, P. J. 1978, Bull. of AAS 10, 506.

Rosenberg, F. D., Eyles, C. J., Skinner, G. K., and Willmore, A. P. 1975, Nature 256, 628.

Ross, R. R., Weaver, R. and McCray, R. 1978, Ap. J. 219, 292.

Rothschild, R., Boldt, E., Holt, S., Serlemitsos, P., Garmire, G., Agrawal, P., Riegler, G., Bowyer, S. and Lampton, M. 1978, Space Science Inst., in press.

Ryter, C., Cesarsky, C. J., and Audouze, J. 1975, Ap. J. 198, 103.

Serlemitsos, P. J., Boldt, E. A., Holt, S. S., Rothschild, R. E., and Saba, J.L.R. 1975, Ap. J. (Letters) 201, L9.

Trumper, J., Pietsch, W., Reppin, C., and Voges, W. 1978, Ap. J. (Letters) 219, L105.

Wheaton, W. A., Howie, S. K., Goldman, A., Cooke, B. A., and Lewin, W.H.G. 1978, Bull. of AAS 10, 506.

TABLE 1

IRON LINE PARAMETERS

Line Flux	$.054\,^{+.021}_{-.007}$	photons/cm^2 sec
Equivalent Width	$.881\,^{+.340}_{-.110}$	keV
E_{line}	$6.79 \pm .06$	keV
FWHM	$3.8 \pm .3$	keV

FIGURE CAPTIONS

Figure 1 - Ariel 5 All Sky Monitor measurements of the X-ray flux from 4U0115+63 during the transient outburst of January 1978. The open circles represent data taken in the fine resolution mode (typical resolution $\cong 2^o \times 2^o$), for which there is no source confusion. The filled circles refer to data taken in the course resolution (all sky) mode for which the resolution per core memory element is $\sim 8^o \times 8^o$; in this mode there may be minor contributions from other sources. For comparison, the Crab nebula $\cong 1.2\ cm^{-2}s^{-1}$. Data gaps correspond to times when the source is out of the instrument field-of-view or times during fine mode observations of other sky regions. The times of the HEAO-A2 pointed and scanning mode observations are indicated.

Figure 2 - Results of pulse phase analysis of HEAO-A2 pointed data. Curves a, b and c refer to HED III data; curves d, e and f refer to MED data. Error bars represent 1σ statistical errors.

2a, 2d - Intensity profile of 4U0115+63.

2b, 2e - Power law number index versus pulse bin (or phase).

2c, 2f - High energy cutoff parameters for the power law model.

Figure 3 - Power law model fits to the HED III data of bins 2 and 3. The curves on the left show a comparison of model spectra folded through the detector response matrix to the net PHA counts. Curves on the right represent inferred incident spectra.

Figure 4 - The curve on the left is a blackbody fit to the HED III PHA data of bin 5. On the right is the inferred incident spectrum for bin 5 using the blackbody model.

E.A. BOLDT, S.S. HOLT, L.J. KALUZIENSKI, F.E. MARSHALL, S.H. PRAVDO,
L.A. ROSE, R.E. ROTHSCHILD, and P.J. SERLEMITSOS
Code 661, Laboratory for High Energy Astrophysics, NASA/Goddard Space
Flight Center, Greenbelt, MD 20771

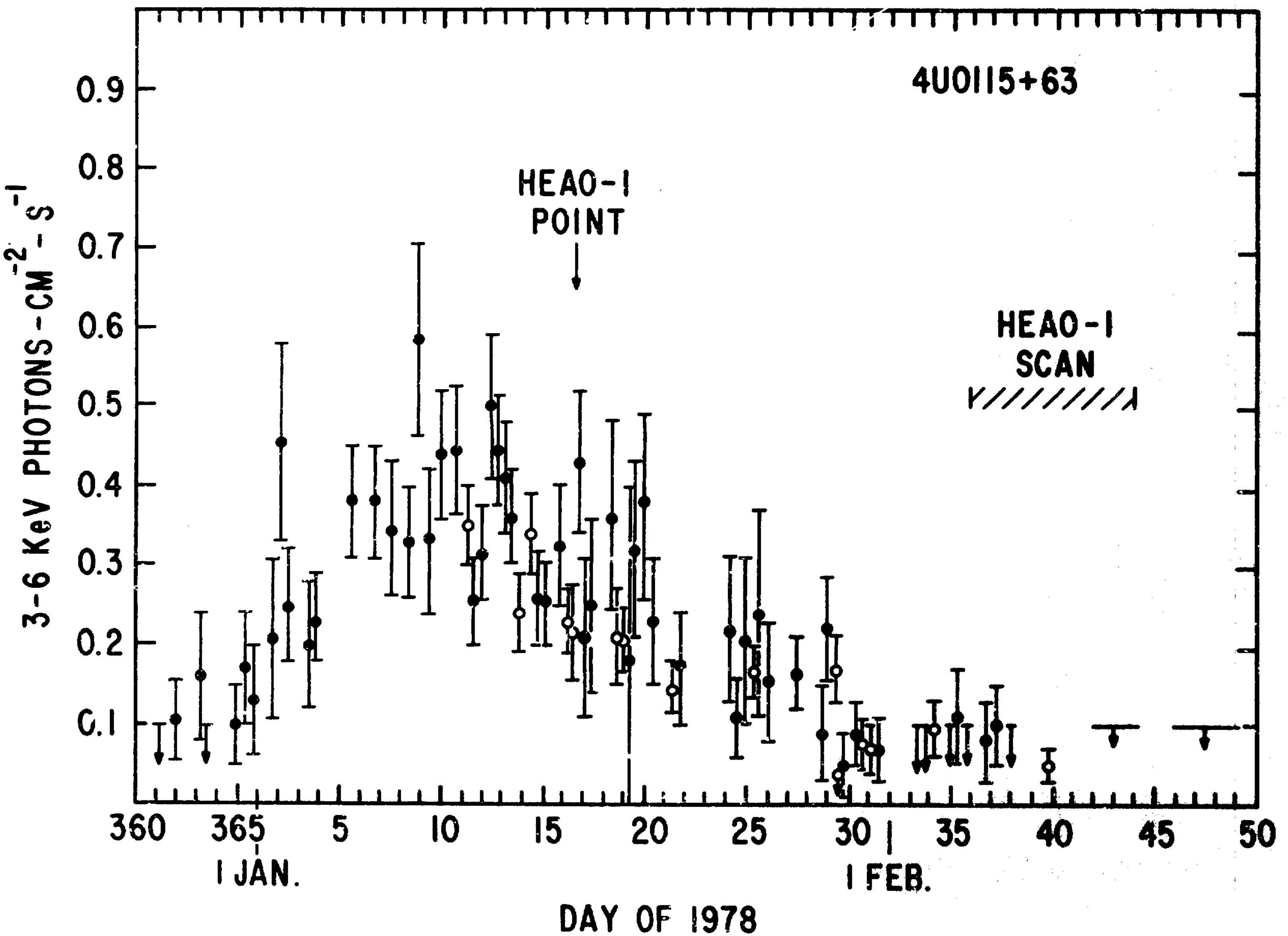
4U0115+63
HEAO-1
POINT
HEAO-1
SCAN
3-6 KeV PHOTONS-CM^{-2}-S^{-1}
0.9
0.8
0.7
0.6
0.5
0.4
0.3
0.2
0.1
360
365
5
10
15
20
25
30
35
40
45
50
1 JAN.
1 FEB.
DAY OF 1978

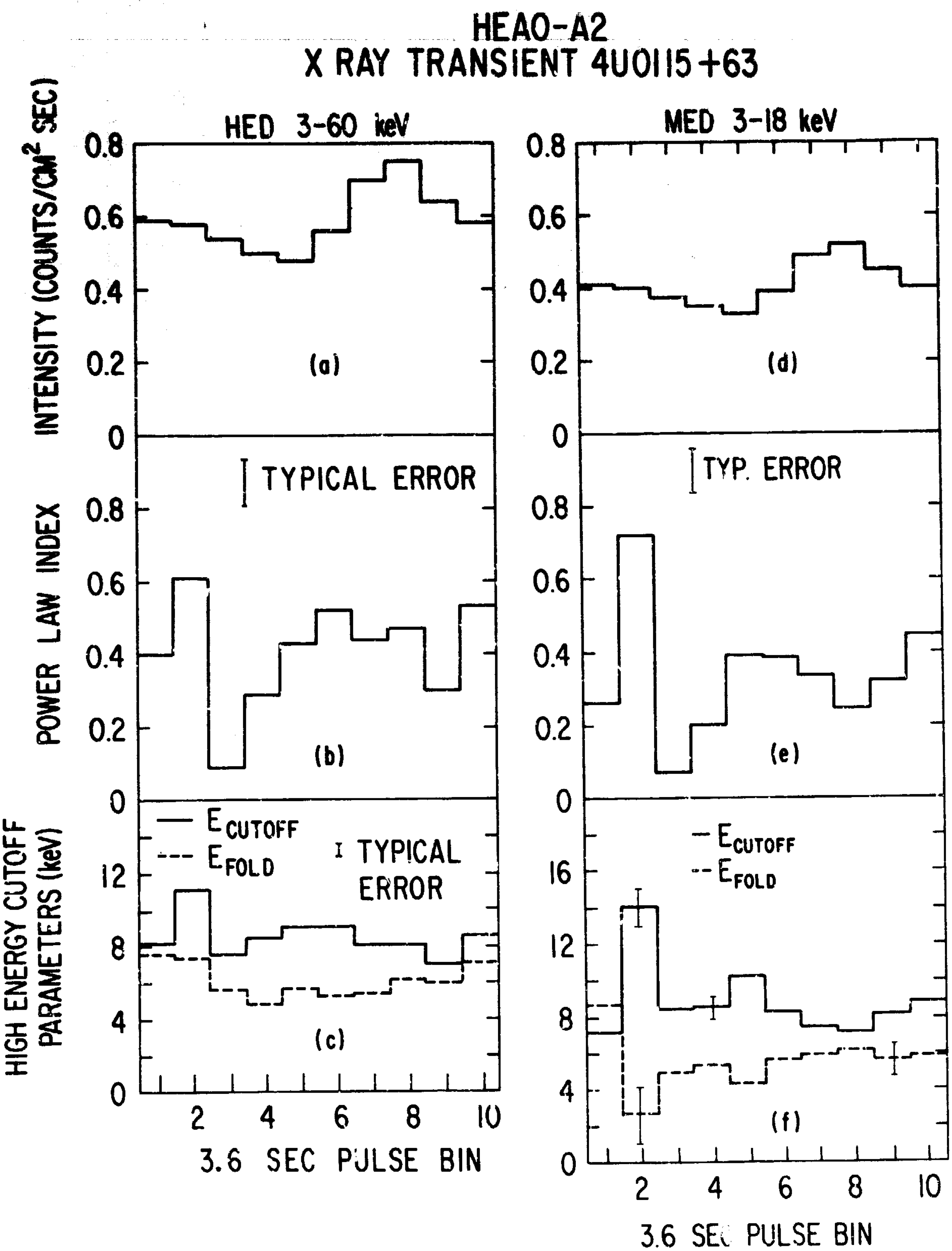

HEAO-A2
X RAY TRANSIENT 4U0115+63
HED 3-60 keV
MED 3-18 keV
INTENSITY (COUNTS/CM² SEC)
POWER LAW INDEX
HIGH ENERGY CUTOFF PARAMETERS (keV)
TYPICAL ERROR
TYP. ERROR
E CUTOFF
E FOLD
(a)
(b)
(c)
(d)
(e)
(f)
3.6 SEC PULSE BIN

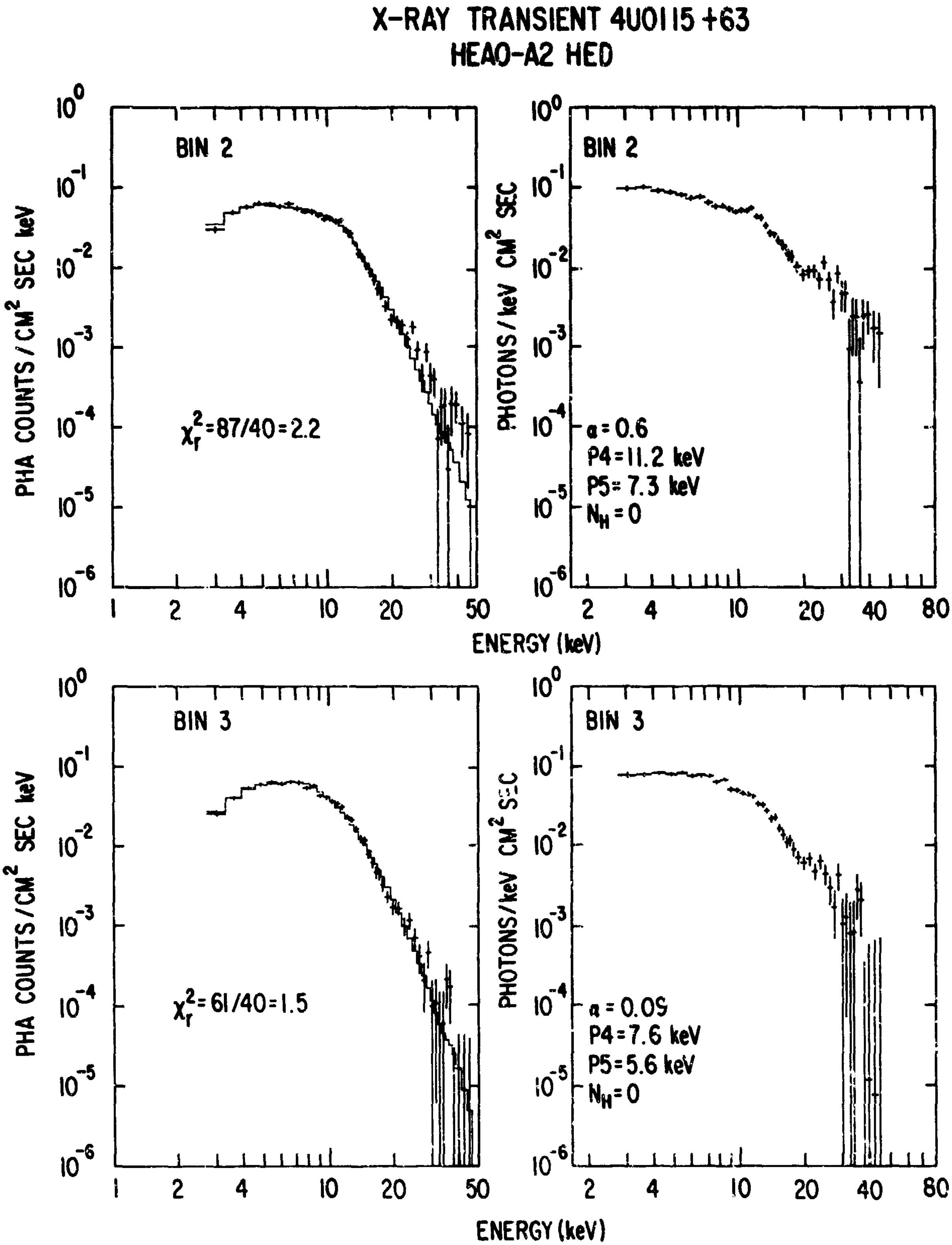

X-RAY TRANSIENT 4U0115+63
HEAO-A2 HED
BIN 2
χ_r^2=87/40=2.2
BIN 2
α=0.6
P4=11.2 keV
P5=7.3 keV
N_H=0
BIN 3
χ_r^2=61/40=1.5
BIN 3
α=0.09
P4=7.6 keV
P5=5.6 keV
N_H=0
PHA COUNTS/CM² SEC keV
PHOTONS/keV CM² SEC
ENERGY (keV)

X-RAY TRANSIENT 4U0115+63
BLACKBODY MODEL
HEAO-A2 HED BIN 5